Identification of Important Residues in Metal−Chelate Recognition by Monoclonal Antibodies†

James B. Delehanty,‡,# R. Mark Jones,‡,¶ Thomas C. Bishop,‡,§,⊥ and Diane A. Blake*,‡,§

Departments of Ophthalmology and Environmental Health Sciences, Tulane University Health Sciences Center, 1430 Tulane Avenue, New Orleans, Louisiana 70112, Division of Basic Pharmaceutical Sciences, Xavier University of Louisiana, New Orleans, Louisiana 70125, and Tulane/Xavier Center for Bioenvironmental Research, New Orleans, Louisiana 70112

Received May 20, 2003; Revised Manuscript Received October 3, 2003

ABSTRACT: The molecular characterization of antibodies directed against metal−chelate complexes will provide important insights into the design and development of radiotherapeutic and radioimaging reagents. In this study, two monoclonal antibodies directed against different metal−chelate complexes were expressed as recombinant Fab fragments. Covalent modification and site-directed mutagenesis were employed to ascertain those residues important in antigen recognition. Antibody 5B2 was raised to a Pb(II)-loaded isothiocyanatobenzyl-diethylenetriamine pentaacetic acid (DTPA)−protein conjugate. The native antibody bound to complexes of Pb(II)−*p*-aminobenzyl-DTPA with an affinity of 4.6×10^{-9} M. A monovalent Fab fragment prepared from the native protein and a bivalent recombinant fragment exhibited comparable affinities for the same Pb(II)−chelate complex, approximately 6-fold lower than that of the intact antibody. Covalent modification and molecular modeling predicted that Lys^{58} in the heavy chain contacted the Pb(II)-chelate ligand. Mutational analysis supported a role for Lys^{58} in ion pair or hydrogen bond formation with the carboxylate groups on the chelate. Antibody E5 was directed toward an isothiocyanatobenzyl-ethylenediamine tetraacetic acid (EDTA)−protein conjugate loaded with ionic Cd(II). The native immunoglobulin recognized Cd(II)−*p*-aminobenzyl-EDTA with an affinity of 8.2×10^{-12} M. A proteolytically derived $F(ab)'_2$ fragment and a bivalent recombinant fragment bound to the same Cd(II)−chelate complex with affinities that were comparable to that of the native antibody. Homology modeling and mutagenesis identified three residues (Trp^{52} and His^{96} in the heavy chain and Arg^{96} in the light chain) that were important for Cd(II)−chelate recognition. His^{96} likely mediates a direct ligation to the Cd(II) ion and Trp^{52} appears to be involved in hydrophobic stacking with the benzyl moiety of the chelator. Arg^{96} appeared to mediate an electrostatic or hydrogen bond to the chelate portion of the complex. These studies demonstrate that antibody recognition of metal−chelate haptens occurs through a limited number of molecular contacts and that these molecular interactions involve both direct ligation between the antibody and the metal ion and interactions between the antibody and the chelator.

Haptens are low molecular weight ligands (usually less than 1000 Da) that have been used as probes to characterize antibody combining sites since Karl Landsteiner first used hapten−protein conjugates to demonstrate the shape-selective nature of antibody−antigen interactions (*1*). Metal−chelate complexes represent a distinct class of hapten ligands, and monoclonal antibodies (mAbs[1]) that recognize these complexes comprise a special subset of metal-binding proteins. Several reports of antibodies that recognize metal−chelate

† This research was supported by the Office of Science (B.E.R.) U.S. Department of Energy, Grant No. DE-FG02-98ER62704 (D.A.B.). Additional support was provided by grants to T.C.B through NSF Cooperative Agreement with the Louisiana Board of Regents (EPS-9720652 NSF/LEQSF 1996-1998-SI-JFAP-04) and by the Office of Naval Research (NO-0014-99-1-0763). J.B.D. was supported in part by a scholarship from the Tulane/Xavier Center for Bioenvironmental Research.

* To whom correspondence should be addressed at Department of Ophthalmology, Tulane University Health Sciences Center. Phone: (504) 584−2478. Fax: (504) 584−2684. E-mail: blake@tulane.edu.

‡ Tulane University Health Sciences Center.

⊥ Xavier University of Louisiana.

§ Tulane/Xavier Center for Bioenvironmental Research.

Present address: Naval Research Laboratory, 4555 Overlook Ave., SW, Washington, DC 20375.

¶ Present address: Sapidyne Instruments Inc., 967 E. Park Center Blvd., Boise, ID 83706.

[1] Abbreviations: BSA, bovine serum albumin; CDR, complementarity determining region; C_H, heavy chain constant domain; C_L, light chain constant domain; CHX-DTPA, trans-cyclohexyldiethylenetriamine-*N*,*N*′,*N*′,*N*′,*N*′′-pentaacetic acid; DTPA, diethylenetriamine-*N*,*N*′,*N*′,*N*′′,*N*′′-pentaacetic acid; DMEM, Dulbecco's modified essential medium; EDTA, ethylenediamine-*N*,*N*,*N*′,*N*′-tetraacetic acid; ELISA, enzyme-linked immunosorbent assay; EOTUBE, 4-[*N*′-2-hydroxyethyl)thioureido]-L-benzyl-EDTA; Fab, fragment antigen binding (monovalent); $F(ab)'_2$, fragment antigen binding (bivalent); Fc, fragment crystallizable; HEPES, (*N*-[2-hydroxyethyl]piperazine-*N*′-[2-ethanesulfonic acid]); HBS, HEPES buffered saline; IgG, immunoglobulin G; ITCBE, 1-(4-isothiocyanatobenzyl)-ethylenediamine-*N*,*N*,*N*′,*N*′-tetraacetic acid; K_d, equilibrium dissociation constant; KLH, keyhole limpet hemocyanin; mAb, monoclonal antibody; NTA, nitrilotriacetic acid; *p*-aminobenzyl-DTPA, *p*-aminobenzyl-diethylenetriamine-*N*,*N*′,-*N*′,*N*′′,*N*′′-pentaacetic acid; PCR, polymerase chain reaction; rms, root-mean-square; SDS−PAGE, sodium dodecyl sulfate−polyacrylamide gel electrophoresis; TMB, 3,3′,5,5′-tetramethylbenzidine; TNBS, trinitrobenzenesulfonic acid; V_H, heavy chain variable region; V_L, light chain variable region.

10.1021/bi034839d CCC: $25.00
Published on Web 11/13/2003

complexes have appeared in the literature. Reardan et al. (*2*) were the first to describe the isolation of a mAb raised to a metal−chelate immunogen. The antibody CHA255 bound with low nanomolar affinity to an In(III)−L-benzyl-EDTA complex while it bound with between 20- and 10 000-fold weaker affinity to L-benzyl-EDTA complexes of 11 other di- and trivalent metals. The mechanism of CHA255's specificity for In(III) was elucidated when the crystal structures of the antibody were solved with either In(III)−L-benzyl-EDTA or Fe(III)−L-benzyl-EDTA in the antibody binding site (*3*). With the In(III) complex in the binding pocket, a histidine in the heavy chain formed a direct coordination to the metal ion. This interaction was not present when the Fe(III) complex was substituted in the binding cleft and the loss of this coordination site was proposed to account for the 20-fold difference exhibited by the antibody for the two metal−chelate complexes. Our laboratory has reported on the isolation of several antibodies directed to metal−chelate complexes. The first, 2A81G5, displayed preferential recognition of EDTA complexes of Cd(II) and Hg(II) (*4*). Modeling studies suggested that a histidine in the heavy chain was involved in the direct coordination of the metal ion. This observation, however, has not been functionally tested by site-directed mutagenesis. 2C12 and 5B2, two other metal−chelate specific antibodies reported by our laboratory, were directed against CHX-DTPA and DTPA complexes of Pb(II) (*5*, *6*). Kinetic data with 2C12 demonstrated that the increased affinity for the Pb(II)−CHX-DTPA complex compared to the metal-free chelator was due to an increase in the antibody's association rate constant when Pb(II) was complexed with the chelate. It was suggested that the observed differential effect of Pb(II) on the antibody's affinity was a result of the antibody's enhanced recognition of a particular octadentate geometry of the chelator. Unfortunately, the lack of available crystal structures or NMR data for Pb(II)−DTPA or Pb(II)−CHX-DTPA has precluded the confirmation of this hypothesis. Jones et al. (*7*) used available crystal data of metal−EDTA complexes to identify structural features of the haptens that were responsible for the differential recognition of the complexes exhibited by two additional monoclonal antibodies generated by our laboratories. These studies showed that antibody affinity correlated well with minimal changes in the molecular shape of the metal−chelate complex. Only cursory regard, however, was given to the molecular nature of the antibody binding site in explaining the affinity of the antibodies for their metal−chelate ligands.

In the present study, we report the molecular characterization of the binding sites of two monoclonal antibodies directed toward different metal−chelate complexes. Equilibrium binding studies and homology modeling allowed us to generate hypotheses regarding the roles of specific amino acid residues in the antibodies' binding sites. In the first instance, covalent modification and site-directed mutagenesis confirmed the importance of a lysine residue in the heavy chain of a mAb with specificity for Pb(II)−chelate complexes. In the second case, mutagenesis experiments confirmed the roles of three residues in the binding site of a mAb directed toward Cd(II)−chelate complexes. We discuss the potential application of our findings to the rational design of antibody reagents to serve as the basis for improved radioimmunotherapy and radioimaging systems.

EXPERIMENTAL PROCEDURES

Materials. Ultrapure bovine serum albumin (BSA) and the IsoStrip mouse monoclonal antibody isotyping kit were obtained from Boehringer Mannheim (Indianapolis, IN). 1-(4-Isothiocyanatobenzyl) ethylenediamine tetraacetic acid (ITCBE), and *p*-aminobenzyl-EDTA were products of CalBiochem Corp. (La Jolla, CA). 1B4M-DTPA was available from previous studies (*5*). Metal ions were atomic absorption grade standards from Perkin-Elmer Corporation (Norwalk, CT). *p*-Aminobenzyl-DTPA was a product of Macrocyclics, Inc. (Dallas, TX). BALB/c inbred mice were purchased from Charles River Laboratories (Wilmington, MA). HEPES, ethylenediamine-*N*,*N*,*N*′,*N*′-tetraacetic acid (EDTA), tissue culture medium, L-glutamine, HAT medium supplement, antibiotics, and goat anti-mouse IgG coupled to horseradish peroxidase were products of Sigma Chemical Co. (St. Louis, MO). Microwell plates for ELISA (flat-bottom, high-binding) and tissue culture plates were purchased from Corning Costar (Cambridge, MA). 3,3′5,5′-Tetramethyl-benzidine (TMB) microwell substrate was a product of Kirkegaard-Perry Laboratories (Gaithersburg, MD). Immobilized protein G resin, the ImmunoPure Fab/F(ab)$'_2$ preparation kit, and the BCA protein assay were obtained from Pierce Chemical Co. (Rockford, IL) and used according to the manufacturer's instructions. Poly-(methyl methacrylate) beads (98 ± 8 μm diameter) were provided by Sapidyne Instruments (Boise, ID). Cy5 conjugates of affinity-purified goat anti-mouse Fc-specific and F(ab)$'_2$-specific antibodies were purchased from Jackson ImmunoResearch Laboratories (West Grove, PA). Restriction enzymes were obtained from New England BioLabs (Beverly, MA) and Promega (Madison, WI). *Pfu* Turbo DNA polymerase was from Stratagene (La Jolla, CA). Lipofectamine 2000 and DMEM tissue culture media were purchased from Invitrogen (Carlsbad, CA). All other materials were obtained as noted in the text.

Protein−Chelate Conjugates. Protein−chelate conjugates were prepared essentially as described in ref *8*. Pb(II)−DTPA−protein conjugates were prepared in a final volume of 1 mL containing 10 mg of BSA, 1.7 mM 1B4M-DTPA, 2.0 mM $Pb(NO_3)_2$, and 47 mM triethylamine in 0.1 M HEPES buffer (pH 9.5). Cd(II)−EDTA−protein conjugates were prepared in a reaction volume of 2 mL containing 20 mg of BSA, 1.36 mM ITCBE, and 1.4 mM Cd(II) in PBS buffer (pH 9.5). The reactions were stirred for 24 h at 25 °C. Unreacted low-molecular weight molecules were removed by buffer exchange using a Centricon-30 device (Amicon, Beverly, MA). The degree of lysine substitution was determined using the trinitrobenzenesulfonic acid method described in ref *9*. The extent of substitution of free lysine residues for the Pb(II) and Cd(II) conjugates was 21.1 and 15.8%, respectively.

Hybridoma Production and Monoclonal Antibody Purification. The isolation and purification of mAb 5B2 has been described in detail elsewhere (*6*). Similarly, the isolation and purification of E5 has also been described in detail in ref *7*. For both 5B2 and E5, the protein concentrations of the purified antibodies were determined using the BCA protein assay kit. The immunoglobulin subclasses were determined by sandwich ELISA using antibodies specific for IgG1, IgG2a, IgG2b, IgG3, IgM, and IgA and the light chains were

Table 1: Binding of Intact IgG, Proteolytic Fragments, and Recombinant Fragments of 5B2 and E5 to Metal−Chelate Complexes[a]

protein	equilibrium dissociation constant (K_d, M)
5B2[b]	
IgG	$4.6 \pm 0.7 \times 10^{-9}$
Fab	$2.8 \pm 0.7 \times 10^{-8}$
rF(ab)$'_2$	$3.1 \pm 1.0 \times 10^{-8}$ [d]
E5[c]	
IgG	$8.2 \pm 3.8 \times 10^{-12}$
F(ab)$'_2$	$1.0 \pm 0.4 \times 10^{-11}$
rF(ab)$'_2$	$1.5 \pm 0.7 \times 10^{-11}$ [e]

[a] K_d values are shown with their 95% confidence intervals. [b] K_d determined for complexes of Pb(II)−*p*-aminobenzyl-DTPA in the presence of an excess of ionic Pb(II) (12 μM) using *p*-aminobenzyl-DTPA as the limiting ligand. [c] K_d determined for complexes of Cd(II)−*p*-aminobenzyl-EDTA in the presence of an excess of *p*-aminobenzyl-EDTA (400 μM) using ionic Cd(II) as the limiting ligand. [d] K_d determined for purified recombinant protein. [e] K_d determined for recombinant protein in concentrated tissue culture supernatant.

isotyped using the IsoStrip antibody isotyping kit according to the manufacturer's protocol.

Molecular Modeling. Molecular models of the heavy and light chain variable domains of 5B2 were constructed according to the canonical structures method detailed in ref *10* using the Swiss-PDB Viewer program (version 3.7) (*11*) and the Swiss-Model automated modeling server at ExPASy (*12*). To ensure proper packing of the heavy chain variable (V_H) and light chain variable (V_L) domains in the resulting models, a crystal structure was identified that contained the V_H and V_L domains in the same antibody. The 5B2 antibody was subsequently modeled upon the crystal structure of antibody N1G9 (PDB ID: 1NGP) (*13*), which was solved to 2.4 Å resolution. The two antibodies exhibited overall sequence identities of 68% in the V_H and 94% in the V_L. Molecular models of the heavy and light chain variable domains of E5 were also constructed from sequence information using the Swiss-Model automated modeling server at ExPASy (*12*). Once the models of the individual chains were calculated, our previous 2A81G5 model (*4*) was used to align the heavy and light chain variable domains of E5. The 2A81G5 model was used for this alignment because the V_H sequences of E5 and 2A81G5 are identical and their V_L sequences differ by only two amino acids in the first framework regions (*4*). For both the E5 and 5B2 models, the canonical structures for the CDR loops as described in refs *10*, *14*, and *15* were identified and fit to the respective loops in our models (root-mean-square deviations reported in Table 2). In all cases, the predicted conformation of the loop backbone atoms was within acceptable limits of known variability.

Due to its extreme length and sequence variability, no canonical structure was identified for CDR H3 of 5B2 (*16*). Therefore, the structure of the parent N1G9 CDR H3 loop was retained throughout the modeling procedure. The sequences were threaded onto their respective templates and the server generated initial models that were used to orient the amino acid side chains of the predicted 5B2 and E5 structures. At positions of sequence identity with the template, the side chain conformation of the template was retained. At positions where the sequences differed, standard rotamer libraries within Swiss-PDB Viewer were queried to identify the most suitable side chain conformer. The stereochemistry of both models was improved by 200 cycles of steepest descent energy minimization. Model quality was assessed with the program WHAT IF (version 19970813-1517) (*17*).

Covalent Modification of Lysine Residues of 5B2. The 5B2 IgG was reacted with trinitrobenzenesulfonic acid (TNBS) in both the presence and absence of Pb(II)−*p*-aminobenzyl-DTPA to assess the ability of the ligand to protect the binding site against lysine modification. 5B2 antibody (75 μg in 750 μL) was incubated with TNBS at a concentration of 170 μM in 0.1 M HEPES buffer (pH 9.5) containing either 3.3 μM Pb(II)−*p*-aminobenzyl-DTPA or no ligand. A control reaction was performed in which the antibody was incubated with 3.3 μM Pb(II)−*p*-aminobenzyl-DTPA in the absence of TNBS. Reactions were stirred at 25 °C for 15 min and terminated by addition of 0.75 mL of 1 mM ethanolamine. Low molecular weight reactants were removed by buffer exchange into HBS (pH 7.4). This was followed by two washes (500 μL each) with 250 μM EDTA in HBS (pH 7.4) to evacuate the binding site. Following buffer exchange into HBS, the samples were normalized to equal protein concentrations using the BCA protein assay. Binding activity in each sample was assayed by indirect ELISA on plates coated with Pb(II)−DTPA−benzyl-BSA essentially as described in

Table 2: Canonical Structure Assignments, Key Residues, and Root Mean Square Deviations for 5B2 and E5 Models

antibody	CDR	canonical structure[a]	key residues present for canonical assignment[b]	rms[g] deviation, Å (acceptable range[c])
5B2	H1	H1−1	T^{24}, G^{26}, F^{27}, I^{29}, M^{34}, R^{94}	0.3−1.1 (0.1−1.2)
	H2	H2−2	P^{52a}, G^{55}, A^{71}	0.3−0.5 (0.3−0.5)
	H3	*d*		*e*
	L1	L1 (λ)-3B	S^{25}, G^{28}, V^{30}, N^{31}, A^{33}, L^{66}, A^{71}, L^{90}	0.8 (0.2−0.8)
	L2	L2 (λ)-1	I^{48}, G^{64}	0.1−0.5 (0.1−0.5)
	L3	L3 (λ)-1A	L^{90}, S^{92}, H^{95}, V^{97}	0.3−0.5 (0.4−1.1)
E5	H1	H1−1	V^{24}, G^{26}, F^{27}, L^{29}, I^{34},N^{94}	0.2−1.1 (0.1−1.2)
	H2	H2−1	G^{55}, K^{71}	0.2 (0.1−0.2)
	H3	H3-short TB[f]	R^{94}, D^{101}	*e*
	L1	L1 (κ)-4	S^{25}, L^{29}, G^{30e}, L^{33}, F^{71}	0.3−0.6 (0.5−0.6)
	L2	L2 (κ)-1	I^{48}, G^{64}	0.1−0.5 (0.1−0.5)
	L3	L3 (κ)-1	Q^{90}, P^{95}, T^{97}	0.2−0.7 (0.1−0.9)

[a] Canonical assignments are according to Morea et al. (*10*). [b] CDR residues are numbered according to the structural numbering in ref *14*; all others are numbered according to Kabat numbering (*33*). [c] Acceptable ranges for individual amino acid side chains in each loop were taken from ref *14*. [d] No canonical assignment was made. [e] No loops of the correct length were available for alignment. [f] Short TB = short torso bulged. [g] rms = root-mean-square.

ref *8*. KinExA analysis (described below) was used to quantify the relative amount of active antibody in each sample by drawing 0.1 μg of total protein over the antigen-coated beads and detecting the bound antibody using a Cy5-conjugated goat anti-mouse polyclonal antibody. Equilibrium dissociation constants were determined using the KinExA and Pb(II)−*p*-aminobenzyl-DTPA as the soluble ligand (described below). The number of modified lysine residues was determined using a value of 1.1×10^4 $M^{-1}cm^{-1}$ for the extinction coefficient of ϵ-trinitrophenyl-α-*N*-acetyllysine at 367 nm.

Production of Proteolytic Fragments of 5B2 and E5. A monovalent Fab fragment of 5B2 and a bivalent F(ab)$'_2$ fragment of E5 were prepared by subjecting the intact IgG to proteolysis with immobilized papain (5B2) or pepsin (E5). The progress of the digestion was monitored by SDS−PAGE followed by Coomassie staining and Western blotting using Fc- and light chain-specific antibodies. The Fc and undigested IgG fragments were removed by passing the digestion reaction over a column of agarose-immobilized protein A.

Cloning, Expression, and Purification of Recombinant Antibodies. The antigen-binding domain of 5B2 was cloned as a bivalent F(ab)$'_2$ fragment (r5B2). The plasmid pFab-CMV (*18*) was used as an intermediate vector for cloning the heavy chain as a V_H-C_H1 fragment. The fragment was cloned into the XhoI-SpeI site of the pFab-CMV vector after polymerase chain reaction (PCR) amplification from hybridoma cDNA using the primers 5B2HCBack-XhoI and 5B2HCFor-SpeI (described in Supporting Information[2]). This placed the fragment in frame with a murine heavy chain leader sequence and the upper portion of the murine IgG_1 hinge (terminating at the first cysteine residue in the hinge). The leader−V_H−C_H1−hinge fragment was amplified from the pFab-CMV vector using sequential amplifications with the backward primer 5B2HCBack-NotI and the forward primers 5B2HCFor and 5B2HCFor-KpnI. This amplification appended the remainder of the murine hinge and the fragment was cloned into the EF-1α promoter site of the vector pBudCE 4.1 (Invitrogen, Carlsbad, CA), placing it in frame with a V5 epitope tag and a hexahistidine affinity tag. The light chain (leader−V_L−Cλ) was amplified using the primers 5B2LCBack-HndIII and 5B2LCFor-XbaI. The forward primer encoded a stop codon that terminated transcription at the terminal serine residue in the light chain. The fragment was cloned into the CMV promoter site of pBudCE 4.1.

E5 was also cloned as a bivalent F(ab)$'_2$ fragment (rE5). The heavy chain (leader−V_H−C_H1−hinge) was cloned from hybridoma cDNA using sequential PCR amplifications with the backward primers E5HCBack and E5HCBack-NotI and the forward primer E5HCFor-KpnI. The light chain (leader−Vκ−Cκ) was cloned using sequential amplifications with the backward primers E5LCBack-1, E5LCBack-2, and E5LCBack-SalI and the forward primer E5LCFor-XbaI. Mutant clones were generated using the QuickChange Site-Directed Mutagenesis kit (Stratagene, La Jolla, CA) and primers encoding the desired mutation. PCR amplifications were performed using Pfu Turbo DNA polymerase, and all cloning manipulations were confirmed by automated DNA sequencing in an institutional facility.

[2] The sequences of all primers are provided in Supporting Information.

Recombinant proteins were expressed by transfection of COS-1 cells (American Type Culture Collection, Manassas, VA). One hundred millimeter tissue culture plates were seeded with 2.5×10^6 cells in growth media (DMEM containing 10% fetal bovine serum) and grown for 20 h. Immediately prior to transfection, culture media was removed and replaced with an equal volume of serum-free DMEM. For transfection, 14 μg of plasmid DNA was mixed with Lipofectamine 2000 reagent (2.5 μL of reagent per μg of DNA) in serum-free DMEM. After incubation at room temperature for 20 min, the mixtures were added to the cells, and the cultures were incubated for 6 h at 37 °C, after which the complexes were removed and replaced with growth media. Expression proceeded for 72 h for 5B2 transfections. Culture supernatants were subjected to buffer exchange into a binding buffer (50 mM NaH_2PO_4, 300 mM NaCl, 20 mM imidazole, pH 8.0). Expressed proteins were applied to a Ni(II)-NTA-agarose affinity chromatography and subsequently eluted with binding buffer containing 300 mM imidazole. Permanently transfected COS-1 cell cultures were established for the recombinant E5 antibody studies by applying Zeocin (200 μg/mL culture media) 72 h after the transfection. The cells were maintained in growth media containing 200 μg/mL Zeocin for 7 days. After subculture, the cells were allowed to recover for 24 h without Zeocin, then selective pressure was reapplied until the next subculture. This process was continued for six weeks, after which the transfected lines were preserved in liquid nitrogen. Culture supernatants from these transfected cells were concentrated before binding studies.

Determination of Equilibrium Dissociation Constants. The KinExA 3000 immunoassay instrument (Sapidyne Instruments, Inc., Boise, ID) was used to measure the equilibrium interactions of the whole IgGs, proteolytic fragments, and recombinant versions of the 5B2 and E5 antibodies with different metal−chelate complexes. The assay format employed was essentially identical to that described previously (*4*, *5*) with the following exceptions.

For binding experiments with 5B2 and its derivatives, the immobilized ligand adsorbed to the beads was Pb(II)−DTPA−benzyl-BSA. Equilibrium dissociation constants (K_d) were determined for Pb(II)−*p*-aminobenzyl-DTPA using concentrations of 0.04, 0.05, and 0.15 μg/mL of intact IgG, Fab, and r5B2, respectively. Binding studies on E5 and its derivatives were conducted using Cd(II)−EDTA−benzyl-BSA as the immobilized ligand. Equilibrium dissociation constants for soluble Cd(II)−*p*-aminobenzyl-EDTA were measured using concentrations of 0.1 μg/mL of intact IgG and 0.05 μg/mL of F(ab)$'_2$ or rE5. The concentrations of metal ions and soluble chelators used are given in the legend to Table 1. For equilibrium reactions containing proteolytic or recombinant fragments of 5B2, BSA was added to a final concentration of 0.1% (w/v) to stabilize the fragments and the instrument bead reservoir was amended with 1 μM metal (Pb(II)) for fragments of 5B2 to ensure that all chelator sites on the immobilized ligand were occupied with metal. These procedures were not required for the analysis of E5 fragments.

Data acquisition was accomplished using a PC interfaced with the KinExA instrument and software distributed by Sapidyne Instruments. Equilibrium dissociation constants were determined from nonlinear regression analysis of the

data using a one-site homogeneous binding model resident within SlideWrite Plus (version 5.0, Advanced Graphics, Inc. Encinitas, CA).

Determination of Recombinant Antibody Binding Activity. Although equilibrium dissociation constants could be determined for purified r5B2 and rE5 using the KinExA, the affinities of the mutants were too low to obtain an adequate signal. Therefore, the comparisons of the binding activities of r5B2 and its mutants were made by indirect ELISA using tissue culture supernatants. rE5 and its mutants were expressed at extremely low levels (1−2 ng/mL). Direct comparisons of the binding activities were therefore performed using concentrated tissue culture supernatants and indirect ELISAs (*8*).

RESULTS

Binding Characterization. The affinities of various forms of the 5B2 and E5 antibodies for metal−chelate complexes were determined by conducting equilibrium binding measurements using a KinExA 3000 immunoassay instrument. The KinExA is a flow spectrofluorimeter that separates and quantifies the free, unbound antibody remaining in equilibrium reaction mixtures of antibody, antigen, and antibody−antigen complexes (*4*, *5*, *19*). A uniform column of microbeads coated with immobilized antigen was deposited into the observation cell of the instrument and was employed to capture those primary antibodies with unoccupied binding sites. Upon exposure of the primary antibodies to a fluorescently labeled anti-mouse secondary antibody, the signal derived from the resulting immobilized immune complex was proportional to the quantity of primary antibody captured on the beads. The binding characteristics determined using the KinExA instrument were those of the soluble reactants in homogeneous solution. In the KinExA technique, the immobilized ligand is merely a tool to capture and quantify a portion of the free, uncomplexed antibody present in a mixture of antibody, ligand, and antibody−ligand complex. The very high effective concentration of immobilized binding sites on the beads (estimated to be ~1 μM from previous experiments (*19*)) dictates that the binding of the limited, soluble antibody (~1 nM in the present study) to the excess immobilized ligand is a pseudo first order process. Under these conditions, only a small but constant percentage of the total uncomplexed antibody (~10%) binds to the immobilized hapten on the beads over a wide range of soluble hapten concentrations. In addition, the time of exposure to the immobilized ligand is very brief (250 ms for the experiments described in this study). For the high affinity binding reactions studied herein, this brief exposure to the immobilized hapten ensures that negligible dissociation occurs during the time of exposure to the beads. As long as these assay conditions are maintained, kinetic exclusion assays provide a linear standard curve for unoccupied (and by difference, occupied) binding sites on soluble antibody regardless of any limiting mass transport or steric hindrance in the binding of antibody to the immobilized ligand.

The structures of the chelators used to characterize the binding sites of the 5B2 and E5 antibodies are shown in Figure 1. The original DTPA immunogen depicts the structure of the chelator−protein conjugate which, when

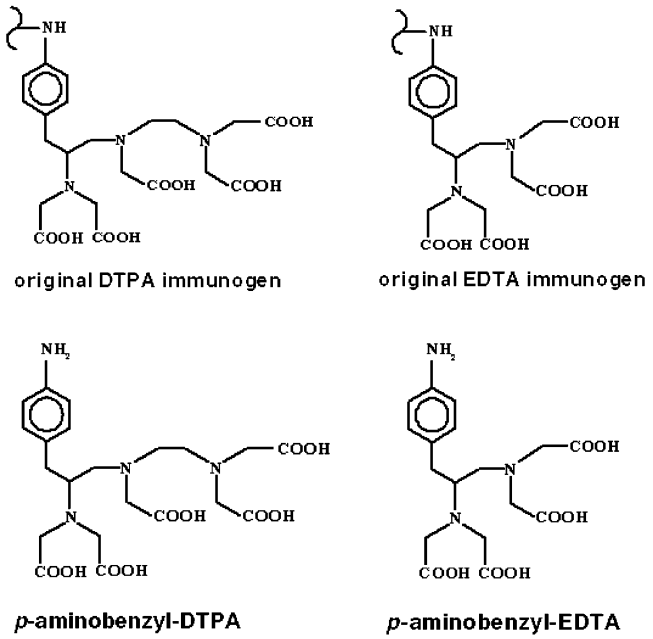

FIGURE 1: Structures of metal chelators. The structures of the metal chelators used in this study are shown. The original immunogens represent isothiocyanatobenzyl derivatives of DTPA and EDTA that were covalently coupled to the carrier protein keyhole limpet hemocyanin.

loaded with ionic Pb(II), was used to elicit the antibody 5B2. This conjugate was formed by reacting isothiocyanatobenzyl-DTPA with keyhole limpet hemocyanin (KLH). Binding studies of the intact 5B2 IgG, a monovalent Fab fragment (5B2 Fab) derived by the proteolytic cleavage of the intact IgG, and a recombinant fragment (r5B2), were conducted with the KinExA using Pb(II)−*p*-aminobenzyl-DTPA as the soluble ligand.

The binding curves shown in Figure 2A were obtained for the binding of the intact 5B2 IgG and its Fab to increasing concentrations of *p*-aminobenzyl-DTPA in the presence of 12 μM ionic Pb(II). An excess concentration of Pb(II) was used to ensure that all chelator molecules existed as a Pb(II)−chelate complex (*20*). Control experiments demonstrated that chelator-free Pb(II) ions at high concentrations had an undetectable effect on the occupation of the antibody binding site (data not shown). The high affinity curve (solid line) was obtained for the intact IgG while the low affinity curve (dashed line) shows the data obtained using the monovalent Fab fragment. From each binding curve, the equilibrium dissociation constant, K_d, was determined from a nonlinear regression fit of the data to the following hyperbolic equation:

$$\text{fraction of occupied binding sites} = \frac{[\text{L}]}{K_d + [\text{L}]} \quad (1)$$

where [L] is the concentration of the soluble ligand. An equilibrium dissociation constant of 4.6×10^{-9} M was determined for the binding of the intact 5B2 IgG to the Pb(II)−*p*-aminobenzyl-DTPA complex. The affinity of the proteolytically derived 5B2 Fab for the same Pb(II)−chelate complex was 2.8×10^{-8} M, a 6.1-fold decrease compared to the intact IgG. The affinity-purified bivalent recombinant fragment, r5B2, bound to the Pb(II)−chelate complex with an affinity of 3.1×10^{-8} M (raw data not shown), a value that was not statistically different from that of the monovalent

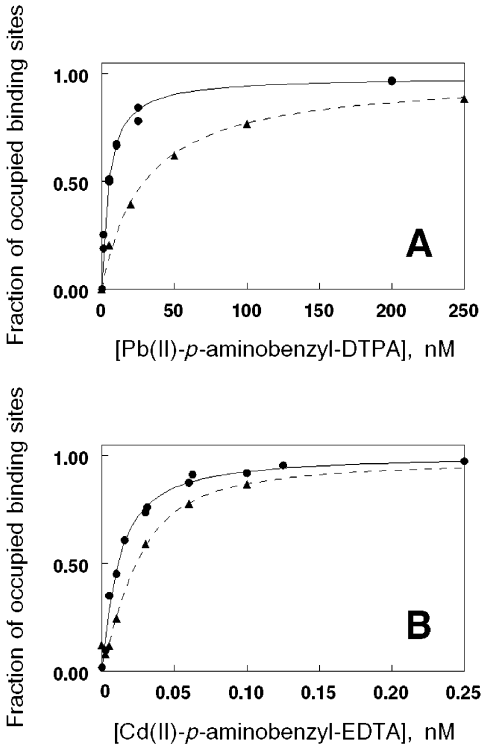

FIGURE 2: Determination of equilibrium dissociation constants for IgG and proteolytic fragments of 5B2 and E5 binding to metal−chelate complexes. (A) concentration dependence of IgG (●) and Fab (▲) of 5B2 binding to *p*-aminobenzyl-DTPA in the presence of 12 μM Pb(II). (B) Concentration dependence of IgG (●) and F(ab)$'_2$ (▲) of E5 binding to Cd(II) in the presence of 400 μM *p*-aminobenzyl-EDTA. Each determination was performed in duplicate. The curves drawn through the data points were generated using eq 1 in the text. Equilibrium dissociation constants are summarized in Table 1.

Fab. These equilibrium binding data are summarized in Table 1. It is worth noting that the values of the dissociation constants measured with the KinExA are independent of antibody valency as the immobilized ligand on the beads separates a constant proportion of uncomplexed antibody in solution in quantifying the concentration of unoccupied antibody binding sites (*19*).

The antibody E5 was elicited in a fashion similar to that employed for the production of the 5B2 antibody (*7*). However, in this case the original immunogen was Cd(II)-loaded isothiocyanatobenzyl-EDTA that was covalently coupled to KLH (Figure 1). Hence, the binding site of the E5 antibody was characterized using soluble complexes of Cd(II)−*p*-aminobenzyl-EDTA. As with 5B2, binding studies were performed on three different forms of the E5 antibody. The binding curves in Figure 2B depict the results of the binding of the intact E5 IgG (solid line) and the proteolytically derived bivalent fragment E5 F(ab)$'_2$ (dashed line) to soluble ionic Cd(II) in the presence of 400 μM *p*-aminobenzyl-EDTA. Control experiments demonstrated that concentrations of the metal-free chelator used in these experiments had no detectable effect on the occupation of the antibody's binding site (data not shown). The intact E5 IgG bound to the Cd(II)−chelate complex with an affinity of 8.2×10^{-12} M. E5 F(ab)$'_2$ recognized the Cd(II)−*p*-aminobenzyl-EDTA complex with a slightly lower affinity, 1.0×10^{-11} M. The bivalent recombinant fragment rE5 also bound to the Cd(II)−chelate complex with an affinity that was comparable to that of the intact IgG, 1.5×10^{-11} M (raw data not shown). These binding data are summarized in Table 1.

The binding characterization of 5B2 and E5 demonstrated that for both antibodies, no differences were observed in the affinities of the recombinant fragments compared to their respective proteolytically derived fragments. Thus, the recombinant fragments could be used as platforms for the investigation of the roles of specific amino acid residues through site-directed mutagenesis experiments.

Molecular Modeling of Antigen Binding Domains. Molecular models of the antigen binding domains of the 5B2 and E5 antibodies were constructed according to previously described canonical structures methods (*10*, *13*, *15*). The identification of the canonical structures of the CDR loops was based upon the length of the loops and the presence of key residues at specific locations in the antibody sequence. This method allows prediction of all three CDRs in the V_L and for CDRs H1 and H2 (and occasionally CDR H3) in the V_H and has correctly described the main chain conformations of CDR loops in blind tests (*13*, *15*). The canonical structure assignments for the CDR loops, the key residues present in the 5B2 and E5 antibody sequences, and the root-mean-square deviations for CDR loops in each model are summarized in Table 2. The energies of the final models were determined to be −11,296 and −12,611 kJ/mol for 5B2 and E5, respectively, using the GROMOS96 implementation of Swiss-PDBViewer (*11*).

Using antibody N1G9 as a template, the structures of all three CDRs in the V_L and CDRs H1 and H2 in the V_H were predicted for 5B2. In a previous crystallographic analysis of a monoclonal antibody's interaction with a metal−chelate antigen, positively charged amino acid side chains were implicated in both ion pair and hydrogen bond interactions with the chelate portion of the ligand (*3*). Figure 3A shows that in the predicted 5B2 binding site, two lysine residues (both in the V_H domain) were in close proximity to the center of the binding pocket. The side chain of Lys^{30} (K30), located in the center of the CDR H1 loop, was predicted to be oriented away from the binding site and did not appear to be in position for antigen recognition. Lys^{58} (K58), however, located within the third framework region (three residues removed from the CDR H2 loop) appeared to have its side chain presented toward the binding site in an orientation for potential ligand binding. We hypothesized, therefore, that Lys^{58} was involved in 5B2's recognition of Pb(II)-chelate complexes via electrostatic interaction or hydrogen bond formation with one of the carboxylate groups on the chelate.

As a result of the high degree of sequence identity between 2A81G5 and E5, several molecular contacts previously suggested as important for the recognition of the Cd(II)−chelate ligand by 2A81G5 (*4*) were investigated for E5. The side chain of His^{96} (H96) in the heavy chain of 2A81G5 was predicted to be in close enough proximity to the Cd(II) ion to form a direct coordination to the metal ion. Additionally, Trp^{52} (W52), also in the heavy chain of 2A81G5, was hypothesized to be involved in a hydrophobic stacking interaction with the phenyl moiety of the chelate. In the E5 model, His^{96} and Trp^{52} were clearly observed to be pointing into the center of the binding pocket in a manner similar to that exhibited by 2A81G5; see Figure 3B. Further, as Arg^{96} (R96) in CDR L3 of the light chain of 2A81G5 was observed to be pointing upward from the rear of the binding site, it

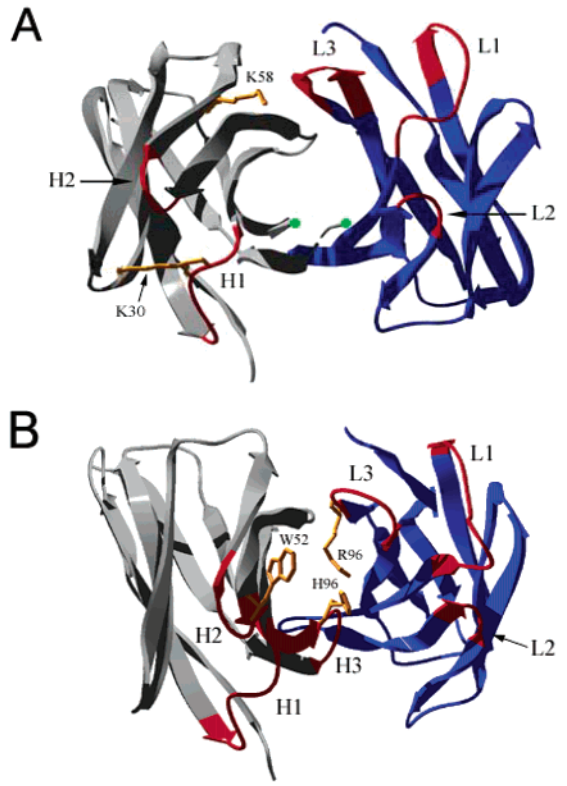

FIGURE 3: Molecular models of the binding sites of 5B2 and E5 antibodies. (A) Model of the 5B2 antigen binding domain. The predicted side chain orientations of lysine residues 30 and 58 (K30 and K58, respectively) in the heavy chain are indicated. The green dots denote the positions where the main chain was broken to remove the CDR H3 loop of the parent template (no structure predicted). (B) Model of the E5 antigen binding domain. The predicted side chain orientations of tryptophan 52 (W52) and histidine 96 (H96) in the heavy chain and arginine 96 (R96) in the light chain are indicated. In both models, the heavy chain is in gray and the light chain is in blue. CDR loops in the heavy (H) and light (L) chains are labeled and are shown in red.

was hypothesized that it could mediate a stabilizing effect through electrostatic or hydrogen bond interactions with the chelate portion of the Cd(II)−chelate complex. A similar stabilizing effect can be realized by R96 in the E5 model.

Covalent Modification of Lysine Residues of 5B2 IgG. To address the importance of lysine residues in 5B2's recognition of Pb(II)−chelate complexes, the lysine residues were covalently modified with the primary amine-specific reagent, trinitrobenzenesulfonic acid (TNBS). Figure 4A shows the results of an indirect ELISA performed after modification of 5B2 with TNBS. Reaction of 5B2 with TNBS in the absence of ligand resulted in a 4-fold decrease in Pb(II)−DTPA−benzyl-BSA binding activity (compared to the unreacted control). However, when the TNBS reaction was performed in the presence of Pb(II)−*p*-aminobenzyl-DTPA, the antibody's binding activity decreased by only 1.4-fold. It was apparent, therefore, that the Pb(II)−chelate ligand protected the binding site against the inhibitory effects of the modification. Spectrophotometric analysis revealed that when reacted with TNBS in the absence of ligand, the 5B2 IgG had an average of six modified lysine residues per protein while the sample that was reacted with TNBS in the presence of ligand had an average of only three modified lysines. Figure 4B shows the KinExA quantification of the relative amounts of active protein in these same samples.

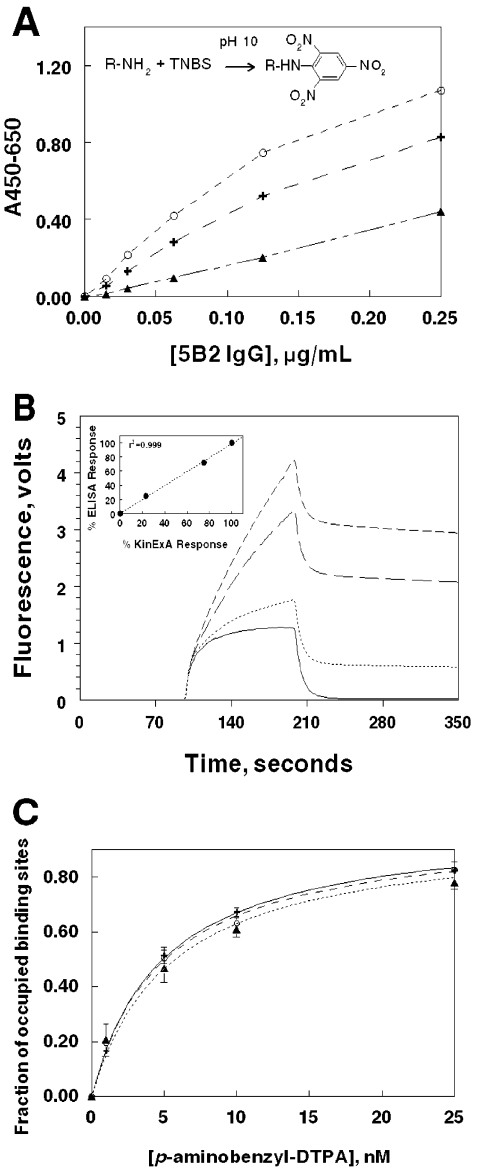

FIGURE 4: The effect of TNBS modification of lysine residues on the Pb(II)−*p*-aminobenzyl-DTPA binding activity of 5B2 IgG. Modification experiments were performed as described in Experimental Procedures using Pb(II)−*p*-aminobenzyl-DTPA as the soluble ligand. (A) Indirect ELISA for the TNBS-modified 5B2 IgG. Data are shown for the following samples: 5B2 incubated with soluble ligand in the absence of TNBS (○), 5B2 incubated with soluble ligand in the presence of TNBS (+), and 5B2 incubated with TNBS in absence of soluble ligand (▲). The inset depicts the reaction mechanism of primary amine modification with TNBS. (B) KinExA quantification of the relative amounts of active IgG present in the reactions described in panel A. Quantification was performed as described in Experimental Procedures. The fluorescent traces represent the amount of active IgG present in the samples as follows: 5B2 + soluble ligand (- - -), 5B2 + soluble ligand + TNBS (− − −), 5B2 + TNBS (•••). The solid trace represents the buffer control. The inset depicts the correlation between the ELISA and KinExA analyses of the samples. (C) Determination of the equilibrium dissociation constants the active 5B2 present in TNBS-modification reactions. Binding experiments were performed as described in Experimental Procedures. Each data point represents the mean ± SD of three independent determinations. Samples and symbols are the same as described in panel A. The equilibrium dissociation constants for each sample are summarized in Table 3.

The inset shows the high degree of correlation between the ELISA response and the KinExA response ($r^2 = 0.999$). The TNBS modification implicated the important role of at least

Table 3: Binding of 5B2 IgG to Pb(II)−*p*-aminobenzyl-DTPA after Modification with TNBS

protective soluble ligand[a]	TNBS[b]	equilibrium dissociation constant (K_d, M)[c]
+	−	$4.9 \pm 0.9 \times 10^{-9}$
+	+	$4.9 \pm 0.3 \times 10^{-9}$
−	+	$5.4 \pm 1.5 \times 10^{-9}$

[a] "+" or "−" indicates that Pb(II)−*p*-aminobenzyl-DTPA (3.3 μM) was present or absent, respectively, in the modification reaction mixture. [b] "+" or "−" indicates that TNBS (170 μM) was present or absent, respectively, in the modification reaction mixture. [c] For all K_d determinations, Pb(II)−*p*-aminobenzyl-DTPA was used as the soluble ligand.

one lysine residue present in the binding site in 5B2's recognition of Pb(II)−DTPA−benzyl-BSA. However, the 4-fold decrease in binding activity observed in the indirect ELISA could have been explained by either of two hypotheses. The decreased binding activity could have been attributed to the homogeneous attenuation of the binding sites of all antibodies present in the sample. Alternatively, the modification could have been heterogeneous, resulting in the ablation of binding activity in only a percentage of the antibody population, while the remaining antibodies were either unmodified or modified at lysine residues not directly involved in binding.

To resolve this, equilibrium dissociation constants were determined for the active antibody present in all three samples. The binding curves shown in Figure 4C were obtained using Pb(II)−*p*-aminobenzyl-DTPA as the soluble ligand. The values of the equilibrium dissociation constants are summarized in Table 3. These data demonstrated that among the active antibody populations present in the three samples, there was statistically no difference in the antibody's affinity for the Pb(II)−chelate ligand.

Characterization of Recombinant Antibody Mutants. The model of the 5B2 binding pocket predicted that the side chain of Lys[58] was in a position for potential ligand binding and the TNBS experiments implicated the involvement of lysines in Pb(II)−chelate recognition. We hypothesized, therefore, that Lys[58] was involved in 5B2's recognition of Pb(II)−chelate complexes through an ion pair or hydrogen bond interaction with one of the carboxylate groups on the chelate. The results of an indirect ELISA using expressed proteins in tissue culture supernatant are shown in Figure 5A. These data demonstrated the differential effects of the mutation of Lys[58] to either Ile (K58I) or to Ala (K58A). Compared to wild-type r5B2, the K58I mutant exhibited a 1.8-fold reduction in its ability to bind to immobilized Pb(II)−DTPA−benzyl-BSA, while the K58A mutant displayed a 3.2-fold decrease in its ability to bind the immobilized ligand. KinExA analysis performed on the proteins present in tissue culture supernatant or the affinity-purified proteins revealed that only the wild-type r5B2 was able to deliver a detectable signal under the flow conditions of the assay system. No signal could be detected for the K58I or K58A mutants even when a 10-fold greater amount of material was applied at a slower flow rate relative to the conditions that yielded strong signals for the wild-type protein (data not shown).

The examination of the possible binding site of E5 revealed that the antibody might recognize its Cd(II)−chelate antigen in a manner analogous to that proposed for antibody 2A81G5 (4). Thus, residues His[96] and Trp[52] in the heavy chain and

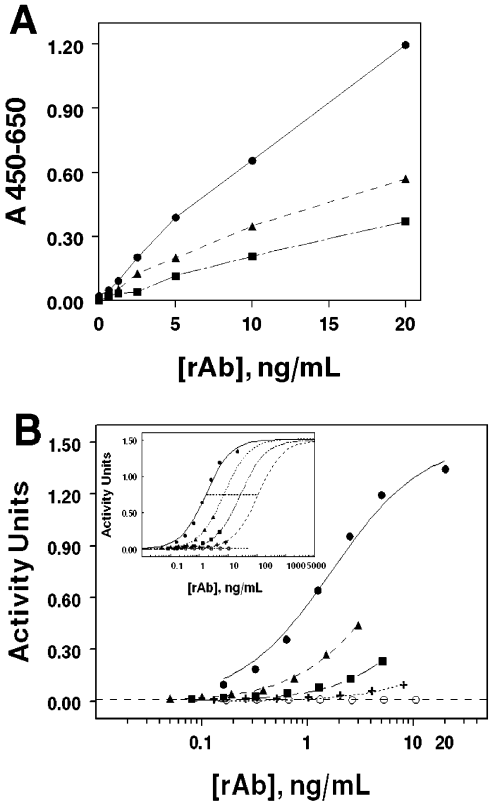

FIGURE 5: The effect of mutation of the binding sites of 5B2 and E5 antibodies on metal−chelate recognition. (A) Indirect ELISA of affinity-purified wild-type r5B2 and mutants. The immobilized ligand was Pb(II)−DTPA−benzyl-BSA. Symbols are wild-type r5B2 (●), K58I (▲), and K58A (■). All samples were normalized to equal protein levels prior to serial dilution in the assay. (B) Indirect ELISA of wild-type rE5 and mutants in concentrated tissue culture supernatants. Cd(II)−EDTA−benzyl-BSA was used as the immobilized ligand. Symbols are wild-type rE5 (●), W52A (▲), R96K (■), R96L (+), and H96L (○). In both panels, each data point represents the mean signal ± SD above the untransfected control. The results shown are representative of assays performed in triplicate.

Arg[96] in the light chain were mutated to assess the effects on the antibody's ability to interact with the Cd(II)−chelate complex. As His[96] was predicted to make a direct coordination to the Cd(II) ion, this residue was mutated to Leu (H96L) to remove the potential for metal ion coordination. The indole ring of Trp[52] was hypothesized to play a role in chelate stabilization through a hydrophobic interaction with the benzyl portion of the Cd(II)−chelate complex. The potential for this interaction was assessed by the mutation of Trp[52] to Ala (W52A). Arg[96] in the light chain, hypothesized to be involved in chelate stabilization, was mutated to either Leu (R96L) or to Lys (R96K).

Figure 5B shows the results of an indirect ELISA performed using concentrated tissue culture supernatants containing wild-type rE5 or mutant proteins. rE5 and its mutants were expressed at extremely low levels (1−2 ng/mL) and the concentrations varied among the expressed proteins. Thus, the determination of activity at a given concentration was not possible for every protein. Therefore, the data were fit to the following equation:

$$A_P = SP/(AU_{50} + P) \quad (2)$$

where P is equal to the antibody concentration in ng/mL, A_P

is the activity units at concentration P, AU_{50} is equal to the amount of antibody (in ng) at half-maximal activity units, and S is equal to the activity units at a saturating concentration of antibody. A_P was determined by indirect ELISA, and P was determined by sandwich ELISA (data not shown). The parameters S and AU_{50} were determined by iterative nonlinear regression using Slidewrite Plus (version 5.0).

The data for wild-type rE5 and the W52A mutant fit well to eq 2, with S values equal to 1.50 ($r^2 = 0.988$) and 1.52 ($r^2 = 0.997$), respectively. The available data for the mutants R96K and R96L could not be fit to eq 2, however, so the upper saturation value was held constant ($S = 1.5$) by a fit of the data to the following equation:

$$A_P = 1.5P/(AU_{50} + P) \quad (3)$$

Eq 3 effectively forced the saturation limit, S, of the curves for R96K and R96L to conform to that observed with the wild-type rE5 and the W52A mutant. This assumption is valid because, when a constant concentration of capture and detection reagents is used in sandwich ELISA, each antibody reaches a constant saturation maximum in the colorimetric assay (data not shown). The inset in Figure 5B shows the extrapolated curves that resulted from a fit of the data for all proteins to an upper saturation limit of 1.5. The extrapolated curves allowed for the comparison of the calculated AU_{50} values. Compared to wild-type E5, the W52A, R96K, and R96L mutants exhibited decreases in binding to immobilized Cd(II)−EDTA-benzyl-BSA of 4-, 16-, and 65-fold, respectively. No activity was detectable for the H96L mutant.

DISCUSSION

The metal−chelate complexes described herein represent a distinct class of low molecular weight (hapten) antigens. Despite their potential utility to serve as the basis for analytical assays to monitor metal contamination in environmental or clinical samples (*8*, *21*, *22*), the number of reports detailing the specific molecular aspects of the antibody binding site that are involved in mediating the metal-chelate recognition process remains limited.

Previous investigations have suggested a role for histidine residues in monoclonal antibody recognition of metal−chelate complexes. Specifically, histidines have been proposed to mediate coordinate covalent bond formation between the antibody binding site and the metal ion of the metal−chelate complex. In X-ray crystallographic analysis of the antigen-binding domain of antibody CHA255 complexed with either In(III) or Fe(III) chelates of thiouriedo-L-benzyl-EDTA, a histidine residue in the third CDR of the heavy chain was implicated in mediating the antibody's preferential recognition of the In(III) chelate over the Fe(III) chelate (*3*). A histidine residue was also proposed to be important in the metal−chelate recognition of a second monoclonal antibody, 2A81G5 (*4*). When the antigen-binding site of 2A81G5 was modeled using the solved crystal structure of CHA255 as a template, histidine at position 96 (His^{96}) in the third CDR of the 2A81G5 heavy chain was found to be less than 0.5 Å apart from the analogous histidine residue in CHA255 and was proposed to make a direct coordination to the cadmium ion in the Cd(II)−EDTA complex. This hypothesis, however, was not directly tested by site-directed mutagenesis. The E5 antibody reported in this study was also raised to a Cd(II)−EDTA−KLH conjugate, and 2A81G5 and E5 displayed a remarkably high degree of sequence identity, differing by only two amino acids in the first framework regions of their light chains. Thus, we hypothesized that they recognized their Cd(II)−chelate ligands through similar mechanisms. In the molecular model of the E5 binding site, which was constructed directly from sequence information, His^{96} in CDR H3 adopted a nearly identical conformation to that observed in 2A81G5; the histidine side chain was oriented toward the center of the binding pocket. When His^{96} was mutated to Leu (H96L), the ability of the E5 antibody to recognize the Cd(II)−chelate complex was completely abrogated, providing convincing evidence of the role of His^{96} in mediating a direct ligation to the cadmium ion. Although this mutation was expected to diminish binding, the total suppression of detectable activity observed in these studies was somewhat surprising. Previous studies (*3*) had suggested that without direct ligation of the His^{96} residue, E5 would retain affinity for metal−chelate complexes but would lose its metal ion specificity. One may rationalize the lack of activity in the H96L mutant by comparing the strength of a coordinate covalent bond (between 10 and 100 kcal/mol) to that of the other noncovalent interactions involved in antibody−antigen interactions (the hydrogen bond strength is ∼4 kcal/mol). In these metal−chelate specific antibodies, the total number of interactions between the antibody and the hapten is limited by the very small size of the metal−chelate complex (∼10 Å in width). Indeed, in the only crystal structure solved to date (*3*), only five interactions were observed between the hapten and the CHA255 antibody, and the coordinate covalent bond between the metal and the histidine made by far the greatest contribution to the total binding energy.

Although His^{96} plays an instrumental role in the E5 antibody's recognition of its Cd(II)−EDTA antigen, it is unlikely that histidine residues are involved in antibody 5B2's interaction with its Pb(II)−DTPA antigen. Sequence analysis of the 5B2 variable domains revealed the presence of two histidine residues in the light chain (H^{42} in framework 2 and H^{95} in CDR L3). In the molecular model constructed for the 5B2 antigen-binding domain, the side chains of both histidine residues were seen to be oriented away from the binding cleft, and these residues were therefore unlikely to mediate a coordinate bond to the metal ion. Histidine ligation was also irrelevant in the binding of Hg^{2+} in a monoclonal antibody that recognized a glutathione−Hg^{2+} complex (*23*). In this antibody, from hybridoma clone 4A10, an unpaired cysteine residue in one hypervariable region was shown by site-directed mutagenesis to be important in metal ion recognition.

While the mutation of His^{96} in E5 established its role in mediating a direct metal ion ligation, mutational analyses of other amino acids within the binding sites of both the E5 and 5B2 antibodies demonstrated the roles of amino acids involved in stabilizing interactions with the chelate portion of their respective metal-chelate complexes. Interactions of amino acid side chains with the chelate portion of metal−chelate antigens have been suggested in both the CHA255 and 2A81G5 antibodies. In the crystal structure of CHA255, arginine, threonine, and tryprophan side chains were observed to form ion pair and hydrogen bonds to the carboxylate arms

of the EDTA molecule (*3*). In the model of 2A81G5, the indole ring of tryptophan was proposed to be involved in a stabilizing hydrophobic interaction with the phenyl moiety of the antigen (*4*). In antibody E5, mutational analysis of Trp^{52} in the heavy chain and Arg^{96} in the light chain provided evidence for their roles in such stabilizing interactions as mutations at these positions resulted in only a decrease in Cd(II)−EDTA binding activity compared to the total inhibition of binding activity seen in the His^{96} mutation. The mutation of Trp^{52} to alanine (W52A) resulted in only a 4-fold decrease in binding activity in indirect ELISA, indicative of the loss of the relatively weak hydrophobic interaction between the antibody and the chelate. The differential inhibitory effect of the mutation of Arg^{96} to either lysine (R96K) or to alanine (R96A) is particularly notable. Mutation of Arg^{96} to lysine, which retained the positive charge and side chain bulk, resulted in a 16-fold decrease in binding activity. Mutation of Arg^{96} to leucine, however, removed both charge and side chain bulk and produced a 64-fold decrease in antigen binding activity. These results support an important role for the long, positively charged side chain of Arg^{96} in mediating an ion pair interaction with the EDTA chelate.

Analogous to the mutations of Arg^{96} in E5, similar inhibitory effects on binding were made by the mutation of Lys^{58} within the heavy chain of 5B2. Molecular modeling predicted that the side chain of Lys^{58} was oriented toward the center of the binding site in a position for potential antigen binding, and covalent modification with TNBS implicated at least one lysine residue as being involved in 5B2's Pb(II)−chelate recognition. Mutation of Lys^{58} to isoleucine (K58I), which removed the positive charge but retained side chain bulk, resulted in only a 1.8-fold decrease in Pb(II)−DTPA binding activity while mutation to alanine (K58A) resulted in a 3.2-fold reduction in binding activity. Further, while the affinity of r5B2 for Pb(II)−*p*-aminobenzyl-DTPA was determined to be 3.1×10^{-8} M, the affinities of the K58I and K58A mutants were estimated to have decreased to at least 1×10^{-6} M. This decrease in affinity corresponds to a change in the free energy of binding ($\Delta\Delta G°$) of at least 2.6 kcal/mol, which is approximately equivalent to the energy of an electrostatic or hydrogen bond (*24*). Thus, these data suggest that Lys^{58} is involved in such an interaction with one of the carboxylate groups of the metal−chelate complex. Experiments are currently underway in our laboratory to determine the contribution of residues within the CDRH3 loop of the 5B2 antibody to metal−chelate recognition. Of particular interest are its extreme length (19 amino acids) and the presence of numerous tyrosine residues throughout the loop.

Here we have conducted the functional characterization of the binding sites of two monoclonal antibodies that exhibit specificity for different metal−chelate complexes. Our results provide evidence that antibody recognition of metal−chelate haptens occurs through only a limited number of molecular contacts. Further, these molecular interactions can involve both direct ligation between the antibody and the metal ion and between the antibody and the chelate portion of the antigen. Recent years have seen advances in the application of pretargeting techniques for enhancing the therapeutic index of radioimmunotherapy for cancer (*25*, *26*) and for the radioimaging of tumors (*27*−*31*) and infectious foci (*32*). Pretargeting strategies have increasingly relied on the use of bispecific antibodies (diabodies) in which one arm of the molecule is directed against the therapeutic target and the other arm is directed toward a metal−chelate complex. A thorough understanding of the molecular interactions of the antibody binding site with the metal−chelate hapten, such as those described herein, will be instrumental to the further development of these promising technologies.

ACKNOWLEDGMENT

The authors gratefully acknowledge the generous gift the pFab-CMV plasmid from Dr P. P. Sanna of Scripps Research Institute.

SUPPORTING INFORMATION AVAILABLE

Primer sequences used for cloning antibodies r5B2 and rE5. This material is available free of charge via the Internet at http://pubs.acs.org.

REFERENCES

1. Landsteiner, K. (1945) *The Specificity of Serological Reactions*, Harvard University Press, Cambridge, MA.
2. Reardan, D. T., Meares, C. F., Goodwin, D. A., McTigue, M., David, G. S., Stone, M. R., Leung, J. P., Bartholomew, R. M., and Frincke, J. M. (1985) *Nature 316*, 265−268.
3. Love, R. A., Villafranca, J. E., Aust, R. M., Nakamura, K. K., Jue, R. A., Major, J. G., Jr., Radhakrishnan, R., and Butler, W. F. (1993) *Biochemistry 32*, 10950−10959.
4. Blake, D. A., Chakrabarti, P., Khosraviani, M., Hatcher, F. M., Westhoff, C. M., Goebel, P., Wylie, D. E., and Blake, R. C., II (1996) *J. Biol. Chem. 271*, 27677−27685.
5. Khosraviani, M., Blake, R. C., II, Pavlov, A. R., Lorbach, S. C., Yu, H., Delehanty, J. B., Brechbiel, M. W., and Blake, D. A. (2000) *Bioconj. Chem. 11*, 267−277.
6. Blake, R. C., II, Delehanty, J. B., Khosraviani, M., Yu, H., Jones, R. M., and Blake, D. A. (2003) *Biochemistry 42*, 497−508.
7. Jones, R. M., Yu, H., Delehanty, J. B., and Blake, D. A. (2002) *Bioconj. Chem. 13*, 408−415.
8. Chakrabarti, P., Hatcher, F. M., Blake, R. C., II, Ladd, P. A., and Blake, D. A. (1994) *Anal. Biochem. 217*, 70−75.
9. Cayot, P., and Tainturier, G. (1997) *Anal. Biochem. 249*, 184−200.
10. Morea, V., Lesk, A. M., and Tramontano, A. (2000) *Methods 20*, 267−279.
11. Guex, N., and Peitsch, M. C. (1997) *Electrophoresis 18*, 2714−2723. (http://www.expasy.org/spdbv/).
12. Peitsch, M. C. (1996) *Biochem.Soc. Trans. 24*, 274−279.
13. Mizutani, R., Miura, K., Nakayama, T., Shimada, I., Arata, Y., and Satow, Y. (1995) *J. Mol. Biol. 254*, 208−222.
14. Al-Lazikani, B., Lesk, A. M., and Chothia, C. (1997) *J. Mol. Biol. 273*, 927−948.
15. Morea, V., Tramontano, A., Rustici, M., Chothia, C., Lesk, A. M. (1998) *J. Mol. Biol. 275*, 269−294.
16. Chothia, C., Lesk, A. M., Tramontano, A., Levitt, M., Smith-Gill, S. J., Air, G., Sheriff, S., Padlan, E. A., Davies, D., and Tulip, W. R. (1989) *Nature 342*, 877−883.
17. Vriend, G. (1990) *J. Mol. Graphics 8*, 52−56.
18. Sanna, P. P., Samson, M. E., Moon, J. S., Rozenshteyn, R., De Logu, A., Williamson, R. A., and Burton, D. R. (1999) *Immunotechnology 4*, 185−188.
19. Blake, R. C., II, Pavlov, A. R., and Blake, D. A. (1999) *Anal. Biochem. 272*, 123−134.
20. Martell, A. E., and Smith, R. M. (1998) in NIST Critically Selected Stability Constants of Metal Complexes, version 5.0.
21. Wylie, D. E., Carlson, L. D., Carlson, R., Wagner, F. W., and Schuster, S. M. (1991) *Anal. Biochem. 194*, 381−387.
22. Darwish, I. A., and Blake, D. A. (2001) *Anal. Chem.* 73, 1889−1895.
23. Westhoff, C. M., Lopez, O., Goebel, P., Carlson, L., Carlson, R. R., Wagner, F. W., Schuster, S. M., and Wylie, D. E. (1999) *Proteins 37*, 429−440.

24. Segel, I. H. (1976) *Biochemical Calculations*, 2nd ed., John Wiley & Sons, New York.
25. Sharkey, R. M., McBride, W. J., Karacay, H., Chang, K., Griffiths, G. L., Hansen, H. J., and Goldenberg, D. M. (2003) *Cancer Res. 63*, 354−363.
26. DeNardo, S. J., DeNardo, G. L., DeNardo, D. G., Xiong, C. Y., Shi, X. B., Winthrop, M. D., Kroger, L. A., and Carter, P. (1999) *Clin. Cancer Res. 5*, 3113s−3218s.
27. Boerman, O. C., Kranenborg, M. H., Oosterwijk, E., Griffiths, G. L., McBride, W. J., Oyen, W. J., de Weijert, M., Oosterwijk-Wakka, J., Hansen, H. J., and Corstens, F. H. (1999) *Cancer Res. 59*, 4400−4405.
28. Kilvenyi, G., Shuhmacher, J., Patzelt, E., Hauser, H., Matys, R., Moock, M., and Maier-Borst, W. (1998) *J. Nucl. Med. 39*, 1769−1776.
29. Shuhmacher, J., Kilvenyi, G., Kaul, S., Henze, M., Matys, R., and Hauser, H., Clorius, J. (2001) *Nucl. Med. Biol. 28*, 821−828.
30. Karacay, H., McBride, W. J., Griffiths, G. L., Sharkey, R. M., Barbet, J., Hansen, H. J., and Goldenberg, D. M. (2000) *Bioconj. Chem. 11*, 842−854.
31. Gestin, J. F., Loussouarn, A., Bardies, M., Gautherot, E., Gruaz-Guyon, A., Sai-Maurel, C., Barbet, J., Curtet C., Chatal, J. F., and Faivre-Chauvet, A. (2001) *J. Nucl. Med. 42*, 146−153.
32. Boerman, O. C., van Eerd, J., Oyen, W. J., and Corstens, F. H. (2001) *J. Nucl. Med. 42*, 1405−1411.
33. Kabat, E. A., Wu, T. T., Perry, H. M., Gottesman, K. S., and Foeller, C. (1991) Public Health Service, NIH, Washington, DC.

BI034839D